

A SWI/SNF-related autism syndrome caused by *de novo* mutations in *ADNP*

Céline Helsmoortel¹, Anneke T Vulto-van Silfhout^{2,16}, Bradley P Coe^{3,4,16}, Geert Vandeweyer^{1,5}, Liesbeth Rooms¹, Jenneke van den Ende⁶, Janneke H M Schuurs-Hoeijmakers², Carlo L Marcelis², Marjolein H Willemsen², Lisenka E L M Vissers², Helger G Yntema², Madhura Bakshi⁷, Meredith Wilson⁸, Kali T Witherspoon^{3,4}, Helena Malmgren⁹, Ann Nordgren⁹, Göran Annerén¹⁰, Marco Fichera^{11,12}, Paolo Bosco¹³, Corrado Romano¹⁴, Bert B A de Vries^{2,15}, Tjitske Kleefstra^{2,15}, R Frank Kooy¹, Evan E Eichler^{3,4} & Nathalie Van der Aa^{1,6}

Despite the high heritability of autism spectrum disorders (ASD), characterized by persistent deficits in social communication and interaction and restricted, repetitive patterns of behavior, interests or activities¹, a genetic diagnosis can be established in only a minority of patients. Known genetic causes include chromosomal aberrations, such as the duplication of the 15q11-13 region, and monogenic causes, as in Rett and fragile-X syndromes. The genetic heterogeneity within ASD is striking, with even the most frequent causes responsible for only 1% of cases at the most. Even with the recent developments in next-generation sequencing, for the large majority of cases no molecular diagnosis can be established²⁻⁷. Here, we report ten patients with ASD and other shared clinical characteristics, including intellectual disability and facial dysmorphisms caused by a mutation in *ADNP*, a transcription factor involved in the SWI/SNF remodeling complex. We estimate this gene to be mutated in at least 0.17% of ASD cases, making it one of the most frequent ASD-associated genes known to date.

Recent developments in next-generation sequencing (NGS), in particular whole-exome sequencing (WES), have substantially increased our insights into the genetic causes of neurodevelopmental disorders. By trio analysis of patients with intellectual disability, a causal *de novo* mutation can be identified in 16–50% of cases⁸⁻¹¹. Interestingly, intellectual disability shows a high comorbidity with ASD, which is present in up to 40% of intellectual disability cases and may be caused by defects in the same genes or pathways¹²⁻¹⁴.

This observation prompted the analysis of existing ASD cohorts with WES^{2,3,5,6,15}. Although mutations were identified in patients with ASD, most mutations seem to be unique, and recurrently mutated genes are scarce¹⁶.

In an initial cohort of ten patients with intellectual disability, ASD and facial dysmorphisms, we identified a patient with a *de novo* mutation in the transcription factor–encoding gene *ADNP* using WES (Supplementary Fig. 1). *De novo* loss-of-function mutations in this gene had previously been identified in two patients by WES² and targeted resequencing¹⁶ of patients with ASD. In those studies, however, the causal relationship did not reach locus-specific significance. On the basis of these initial findings and the association of *ADNP* with neuronal cell differentiation and maturation¹⁷, as well as the cognitive abnormalities observed in a mouse model¹⁸, we considered *ADNP* a strong candidate gene. We subsequently identified 3 mutations in *ADNP* in 240 patients from 3 independent WES studies (Table 1). Next, we targeted *ADNP* using molecular inversion probes (MIPs) or high-resolution melt curve analysis (HRM) in a cohort of 2,891 patients with syndromic ASD and identified 4 more patients with mutations in this gene. In total, 10 mutations were found in 5,776 patients. For nine patients the parents were available for testing, and in each case the mutation appeared *de novo* (Table 1). We found no additional nonsynonymous *de novo* variants. Neither did we find X-chromosomal, compound or homozygous variants in genes known to be associated with intellectual disability or ASD. Autism and comorbidity with mild to severe intellectual disability is a consistent feature in all patients (Table 2 and Supplementary Note). Other frequent findings include hypotonia, feeding problems in infancy and

¹Department of Medical Genetics, University of Antwerp, Antwerp, Belgium. ²Department of Human Genetics, Nijmegen Centre for Molecular Life Sciences, Institute for Genetic and Metabolic Disease, Radboud University Medical Center, Nijmegen, The Netherlands. ³Department of Genome Sciences, University of Washington School of Medicine, Seattle, Washington, USA. ⁴Howard Hughes Medical Institute, University of Washington, Seattle, Washington, USA. ⁵Biomedical informatics research center Antwerpen (Biomina), Department of Mathematics and Computer Science, University of Antwerp, Edegem, Belgium. ⁶University Hospital Antwerp, Antwerp, Belgium. ⁷Department of Genetic Medicine, Westmead Hospital, Sydney, Australia. ⁸Department of Clinical Genetics, Children's Hospital at Westmead, Westmead, Australia. ⁹Clinical Genetics Unit, Department of Molecular Medicine and Surgery, Karolinska Institutet, Stockholm, Sweden. ¹⁰Department of Women's and Children's Health, Uppsala University, Uppsala, Sweden. ¹¹Unit of Neurology, I.R.C.C.S. Associazione Oasi Maria Santissima, Troina, Italy. ¹²Medical Genetics, University of Catania, Catania, Italy. ¹³Laboratory of Cytogenetics, I.R.C.C.S. Associazione Oasi Maria Santissima, Troina, Italy. ¹⁴Unit of Pediatrics and Medical Genetics, I.R.C.C.S. Associazione Oasi Maria Santissima, Troina, Italy. ¹⁵Donders Institute for Brain, Cognition and Behaviour, Radboud University Medical Center, Nijmegen, The Netherlands. ¹⁶These authors contributed equally to this work. Correspondence should be addressed to N.V.d.A. (nathalie.vanderaa@uza.be) or R.F.K. (frank.kooy@uantwerpen.be).

Received 12 November 2013; accepted 23 January 2014; published online 16 February 2014; doi:10.1038/ng.2899

Table 1 Summary of mutations, detection methods and cohorts compositions for the reported patients

Patient ID	Origin	Screening method	Cohort composition	Cohort size	Mutation in genomic DNA (chr. 20)	Mutation in cDNA (NM_015339.2)	Protein change	Mutation type	Inheritance
1	111294	WES	Moderate to severe intellectual disability and/or autism and dysmorphic features	10	g.49508752_49508755delTTTA	c.2496_2499delTAAA	p.Asp832Lysfs*80	Frameshift	<i>De novo</i>
2	11-08612	WES	Nonsyndromic severe intellectual disability	100	g.49510040G>T	c.1211C>A	p.Ser404*	Nonsense	<i>De novo</i>
3	12130.p1	WES ^{2,16}	ASD from the Simon Simplex Collection	189	g.49510028_49510029delTT	c.1222_1223delAA	p.Lys408Valfs*31	Frameshift	<i>De novo</i>
4	1050237	WES	Nonsyndromic severe intellectual disability	95	g.49509086_49509098delATT TGCTCGTAAG	c.2153_2165delCTTAC GAGCAAA	p.Thr718Glyfs*12	Frameshift	<i>De novo</i>
5	3061-08D	WES	Moderate to severe intellectual disability and/or autism and dysmorphic features	45	g.49509094G>C	c.2157C>G	p.Tyr719*	Nonsense	<i>De novo</i>
6	122793	HRM	Autism	148	g.49508757_49508760delTTAA	c.2491_2494delTTAA	p.Lys831Ilefs*81	Frameshift	<i>De novo</i>
7	07-06960	MIPs	Intellectual disability and/or autism	2,743	g.49508443delG	c.2808delC	p.Tyr936*	Frameshift	<i>De novo</i>
8	2376	MIPs	Intellectual disability and/or autism	2,743	g.49508757_49508760delTTAA	c.2491_2494delTTAA	p.Lys831Ilefs*81	Frameshift	<i>De novo</i>
9	2533	MIPs	Intellectual disability and/or autism	2,743	g.49509321G>A	c.1930C>T	p.644Arg*	Nonsense	Parents not available
10	13545.p1	MIPs ¹⁶	ASD from the Simon Simplex Collection	2,446	g.49509094_49509095insT	c.2156_2157insA	p.Tyr719*	Frameshift	<i>De novo</i>

All genomic coordinates relate to genome build GRCh37. WES, whole-exome sequencing; HRM, high-resolution melting; MIPs, molecular inversion probes. Patients 7, 8 and 9 are from the same cohort of 2,743 patients.

congenital heart defects. A seizure disorder was noted in two patients. Additional neuropsychiatric features are relatively common, including attention deficit/hyperactivity disorder, anxiety disorder and obsessive compulsive behavior. Dysmorphic features include a prominent forehead, high hairline, eversion or notch of the eyelid, broad nasal bridge, thin upper lip and smooth/long philtrum (**Fig. 1**).

All mutations are heterozygous frameshift or nonsense variants in the 3' end of the last exon of *ADNP* and result in a premature termination codon (**Table 1**). None were present in the 1000 Genomes Project¹⁹, in 1,728 MIP-sequenced unaffected siblings from the Simons Simplex Collection or in 192 HRM-analyzed chromosomes from healthy Belgian controls. Putative truncating mutations for *ADNP* are in fact rare. Only one nonsense mutation encoding p.Gln361* upstream of all our mutations was reported in the 13,006 alleles of the Exome Sequencing Project (ESP). An inherited mutation encoding p.Gly1094Profs*5 was identified by MIP sequencing¹⁶, but the reported frameshift affects the ninth amino acid from the C-terminal end of the protein and is not associated with any protein domains. Typically, variations that close to the end of a protein are unlikely to affect function. The frequency of truncating mutations in *ADNP* is significantly higher ($P = 0.001852$, odds ratio = 13.24668, one-sided Fisher's exact test) in patients compared to the ESP and Simons controls. In addition to conducting the case-control analysis, we calculated locus-specific enrichment for truncating variation using a probabilistic model derived from human-chimpanzee fixed difference and sequence context as described¹⁶. Under a *de novo* rate of 1.2 nonsynonymous coding variants per individual, we estimate the probability of detecting eight or more *de novo* truncating events in *ADNP* within our cohort as $P = 2.65 \times 10^{-18}$ (binomial test).

The mutated gene, *ADNP* (chr. 20: 49,506,883–49,547,527, GRCh37/hg19), contains five exons, of which the last three are translated (**Fig. 2**). The protein consists of 1,102 amino acids and contains 9 zinc fingers and 3 other functional domains, including NAP, an 8-amino-acid neuroprotectant peptide (NAPVSIPQ)^{20,21}. Administration of NAP ameliorated the short-term memory deficits in *ApoE* knockout mice, a model for Alzheimer's disease²². In *Adnp*^{+/-} mice, NAP treatment restores learning and memory and reduces neurodegeneration¹⁸. Further downstream, a DNA-binding homeobox domain is present, homologous to the *HOX* gene family homeobox domains (InterPro, EBI). A P*V*L motif, which can bind the HP1 protein, is located just downstream of the homeobox domain. The HP1 protein binds to and mediates the histone H3 lysine 9 trimethylation post-translational modification^{23–25}. The homeobox domain and the HP1-binding motif are responsible for the transcription factor function of *ADNP*.

Almost the complete 1.6-kb sequence spanned by the mutations is conserved in mammals (PhyloP mean = 1.52, s.d. = 1.25) (ref. 26). All mutations result in the loss of at least the 166 last C-terminal amino acids. Strikingly, the identified mutations seem to cluster at specific positions. The 4-bp *de novo* deletions in both patient 6 and 8 are identical, even though these patients are unrelated and were born and live in different countries. This mutation is separated by only one nucleotide from the 4-bp deletion in patient 1. Additionally, the mutations observed in patients 5 and 10 fall within the 13-bp deletion in patient 4. Clustering of *de novo*, rare variants is suggestive of a mutation predisposition mechanism, potentially as a result of a particular local genomic architecture. We found no evidence for the presence of simple or tandem repeats in this region. Mfold analysis (web server for nucleic acid folding and hybridization prediction)²⁷ showed that the clustered 4-bp deletions of patients 1, 6 and 8 are located in the stem of the same short hairpin (**Supplementary Fig. 2**). Hence,

Table 2 Clinical characteristics of the patients with *ADNP* mutations

	Patient 1	Patient 2	Patient 3	Patient 4	Patient 5	Patient 6	Patient 7	Patient 8	Patient 9	Patient 10	Total
Sex	M	F	F	M	M	M	F	M	F	M	
Developmental delay (motor)	+	+	+	+	+	+	+	+	-	+	9/10
Developmental delay (speech)	+	+		+	+	+	+	+	-	+	8/9
Intellectual disability	Mild	Mild	Mild	Severe	Severe	Severe	Mild	Severe	Mild	Severe	10/10
ASD	+	+	+	+	+	+	±	+	±	+	10/10
ADHD	-	-	+	-	-	+	-	-	-	-	2/9
Hypotonia	+	+	+	+	+	+	-	+	-	-	7/9
Growth retardation / short stature	+	-		+	+	-	-	+	+		5/8
Feeding problems	+	+	+	+	-		-	-		+	5/8
Recurrent infections	+	+		-	+	-	-	+	+		5/8
Congenital heart defect	+	+	-	-		-		+	-	-	3/8
Hyperlaxity	+	+		+	+	+	-	-	+		6/8
Obesity		-		-	+	+	-	±	+		4/7
Hypermetropia		+		+	+		+	+	+		6/6
Seizures		+		-	-	+	-	-	-		2/7
Behavior		+	+	-	+		-	+	+		5/7
Insensitivity to pain				-	+	+		-	-		2/5
MRI brain abnormality	+	+	-	+	+	-		+	-	-	5/9
Prominent forehead	+	+		-	+	-	+	+	-		5/8
High hairline	+	+		-	+	+	+	+	+		7/8
Eversion/notch eyelid	+	+		-	-		-	+	-		3/7
Hypertelorism	+	-		-	-	-	-	-	-		1/8
Broad nasal bridge	+	+		+	-	+	-	+	+		6/8
Short nose	-	-		-	-	+	-	-	+		2/8
Thin upper lip		+		+	+	+	+	+	-		6/7
Hand abnormalities	+	+	+	+	-		-	+	+		6/8
Constipation		-		+	+		-	-	-		2/6

±, mildly affected.

we suggest that the underlying mechanism of the mutations may involve a DNA-repair defect following pausing of a replication fork at these hairpins.

Because no exon-exon boundary in the *ADNP* mRNA is present downstream from any of the mutations, nonsense-mediated RNA decay (NMD) is unlikely²⁸⁻³⁰. Indeed, the mutations were present in the cDNA generated from lymphoblastoid cell lines of patients 1, 2, 6 and 8. To quantify the impact of truncating mutations on the expression of *ADNP*, we performed expression analysis. Also included in the expression analysis is a set of selected genes previously shown to interact or to be coregulated with *ADNP*^{18,23,31,32}. The total expression of *ADNP* mRNA was significantly ($P = 0.0101$) increased by 41% in patients 1, 2, 6 and 8 (Table 3 and Supplementary Fig. 3b). A single assay specific for the wild-type but not the mutant *ADNP* allele could be generated for patients 1, 6 and 8 to discriminate between wild-type and mutant mRNA expression. The expression of this *ADNP*^{wt} amplicon was not different from controls, demonstrating that

the excess *ADNP* mRNA in patients corresponds to the mRNA transcribed from the mutant allele. Because *ADNP* expression is under the control of an autoregulatory negative feedback loop³³, the overall upregulation might be a consequence of the inability of the mutant protein to bind the *ADNP* promoter. This suggests deregulation of

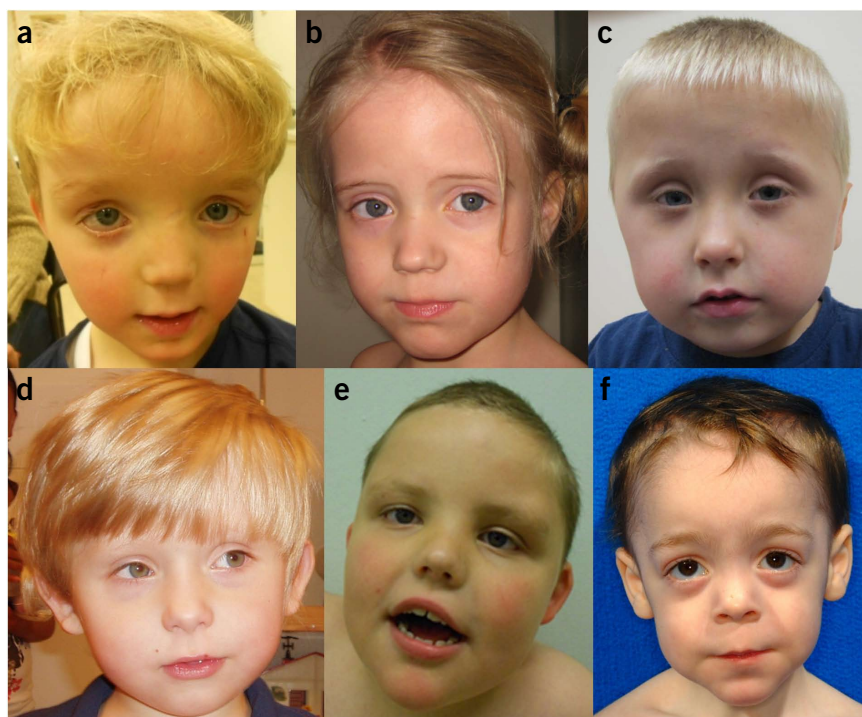
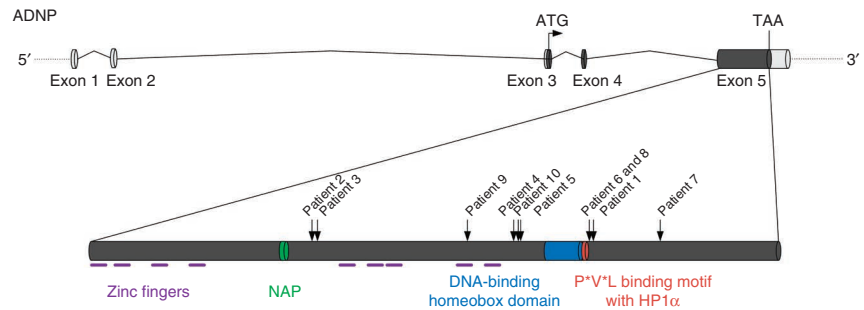


Figure 1 Frontal facial photographs of patients. (a-f) Patients 1 (a), 2 (b), 4 (c), 5 (d), 6 (e) and 8 (f) at young ages. Note the clinical similarities, including a prominent forehead, a thin upper lip and a broad nasal bridge. Consent for the publication of photographs was obtained for these patients (1, 2, 4, 5, 6 and 8).

Figure 2 Schematic overview of the *ADNP* gene structure and functional domains. Identified alterations and corresponding patients in which they were found are indicated by black arrows.



the negative feedback leading to increased expression of *ADNP* mRNA to restore homeostasis. Expression of *ADNP2* (**Supplementary Fig. 3c**) was also significantly ($P = 0.0060$) upregulated in patients, which is in line with the reported high correlation between the expression of *ADNP* and *ADNP2* (ref. 31). Of the other genes reported as differentially expressed in *Adnp*^{-/-} (ref. 23) and *Adnp*^{+/-} (ref. 18) mice (down-regulated: *Cnc*, *Tmpo*, *Plagl2*; upregulated: *Abcf3*), only *PLAGL2* was found to be differentially regulated in our patients (**Supplementary Fig. 3e**). This may be the consequence of differences in tissue and developmental stage between the knockout mice and the human cell lines. Expression of *TP53*, reported to be upregulated in HT29 cells incubated with *ADNP* antioligodeoxynucleotide³², was significantly ($P = 0.0003$) increased (**Supplementary Fig. 3g**), possibly as a result of augmented cellular stress due to an overall deregulation of genes under the transcriptional control of *ADNP*.

ADNP has multiple cellular functions that seem compatible with the clinical presentation of our patients. A role in neuronal cell differentiation and maturation was suggested after observing a substantial decrease in the number and size of embryoid bodies and the number of neurites after knockdown of *ADNP* with short hairpin RNA (shRNA) in P19 cells¹⁷. Furthermore, *Adnp*^{-/-} mice are not viable owing to failure of neural-tube closure, whereas *ADNP*^{+/-} mice show tauopathy, neuronal cell death and abnormalities in social behavior and cognitive functioning^{18,34}. The severity of the phenotype in our cohort varies, but all patients show various degrees of ASD and all are intellectually disabled. Dysmorphic features vary from patient to patient, but a prominent forehead, broad nasal bridge, thin upper lip and smooth philtrum are frequently present. Cardiac, brain and behavioral abnormalities are more frequent in our patients than in the general population. At the moment, there are no indications of a correlation between the individual mutations and clinical presentation. The mutations in patients 6 and 8 are identical and differ only by a single amino acid from the mutation in patient 1. Yet, these three patients do not share more clinical characteristics with each other than with other patients. However, at this moment, it is not possible to draw firm conclusions on a possible genotype-phenotype correlation owing to the small sample size. No patients with a pure

deletion of *ADNP* have been reported. In our own databases and in DECIPHER³⁵, five deletions with sizes of 313 kb–3.31 Mb, taking away 5–23 genes including (part of) *ADNP*, have been described. In the four cases where the parents were tested, the deletion was *de novo*. The patients with *ADNP* deletions all share some clinical characteristics with the patients reported here, carrying truncating mutations (**Supplementary Fig. 4** and **Supplementary Table 1**).

The C-terminal part of *ADNP* directly interacts with ARID1A, SMARCA4 and SMARCC2, three essential components of the BAF complexes, the functional eukaryotic equivalent of the SWI/SNF complex in yeast that is involved in the regulation of gene expression³⁶. These ATP-dependent chromatin remodeling complexes consist of 15 subunits, including one of both ATPase core subunits SMARCA4 or SMARCA2 (ref. 37). A switch of complex composition is essential for the initiation of post-mitotic activity-dependent dendritic outgrowth and axonal development. This transition of neural progenitor cells to mature neurons occurs in all neurons and highlights the fundamental role of BAF complexes in neural development³⁸. Notably, mutations in patients with intellectual disability have been reported in six components of these complexes (*SMARCB1*, *SMARCA4*, *SMARCA2*, *SMARCE1*, *ARID1A* and *ARID1B*). The phenotype associated with mutations in these genes ranges from nonsyndromic intellectual disability with hypotonia and speech delay to recognizable syndromes such as the Coffin-Siris syndrome and Nicolaides-Baraitser syndrome. These disorders are sometimes referred to as ‘SWI/SNF-related intellectual disability syndromes’ (refs. 39–41). It has been proposed that the syndromic features might be explained by the role of BAF complexes in developmental processes in the affected tissues⁴². It is believed that most reported mutations in these genes have a dominant-negative effect on the functioning of the BAF complex as a whole^{43–46}. As we were able to detect mutant RNA in our patients, we hypothesize that the mutant *ADNP* protein competes with the wild-type protein in an aberrant interaction with the BAF complex. Wild-type *ADNP* directly binds target genomic regions and mediates the recruitment of the BAF complex through the C-terminal end. Hence, it can be hypothesized that the mutant protein with an altered C-terminal structure will hamper the recruitment of the BAF complex, while it still occupies DNA binding sites. This will lead to a diminished functionality of the complex and ultimately to deregulation of several cellular processes.

In summary, we identified a recurrent SWI/SNF-related ASD syndrome, caused by mutations in *ADNP*. These findings expand the phenotypic spectrum of SWI/SNF-related disorders, several of which are caused by mutations in direct interaction partners of *ADNP*. Mutations in *ADNP* may explain the etiology of 0.17% of patients with ASD (95% binomial confidence interval: 0.083–0.32%) and thus constitute one of the most frequent known causes of autism. Our findings will increase the diagnostic yield in this population,

Table 3 Real-time quantitative expression analysis of mRNA from Epstein-Barr virus (EBV)-transformed lymphoblastoid cell lines of patients 1, 2, 6 and 8 compared to eight control samples

Gene	Relative expression (%)	s.e.m.	<i>P</i> value	Significance
<i>ABCF3</i>	94.03	14.31	0.6507	
<i>ADNP</i>	141.67	13.4	0.0101	*
<i>ADNP2</i>	148.52	17.58	0.0060	**
<i>ADNPwt</i>	74.28	4.14	0.0729	
<i>CCNC</i>	87.98	6.72	0.2857	
<i>PLAGL2</i>	153.49	21.4	0.0040	**
<i>TMPO</i>	80.26	11.24	0.2462	
<i>TP53</i>	164.81	6.17	0.0003	***

* $P < 0.05$, ** $P < 0.01$, *** $P < 0.001$, according to linear mixed models.

and studies on the role of *ADNP* in development may raise hope for treatment of these patients in the long term.

URLs. Clinical information, <http://www.adnpgene.com>; Galaxy pipeline, <http://biominavm-galaxy.biomina.be/galaxy/u/geert-vandeweyer/w/adnp>; VariantDB, <http://www.biomina.be/app/variantdb>; Real-time PCR design tool, <http://biomina.be/apps/qpcr-primers>; Exome Variant Server, <http://evs.gs.washington.edu/EVS/>.

METHODS

Methods and any associated references are available in the [online version of the paper](#).

Note: Any Supplementary Information or Source Data files are available in the online version of the paper.

ACKNOWLEDGMENTS

This work was funded by the Belgian National Fund for Scientific Research-Flanders (FWO) to G.V. and R.F.K., the Special Research Fund of the University of Antwerp (Bijzonder Onderzoeksfonds (BOF-IWT)) to C.H., by grants from the Dutch Organization for Health Research and Development (917-86-319 and 40-00812-98-12109 to B.B.A.d.V. and 907-00-365 to T.K.), the EU-funded GENCODYS project (EU-7th-2010-241995 to A.T.V.-v.S., B.B.A.d.V. and T.K.), Simons Foundation Autism Research Initiative award (SFARI191889EE to E.E.E.) and NIH (MH101221 to E.E.E.). We acknowledge R. Pettinato and M. Elia for the first enrolling of patients 8 and 9, respectively, and J. Shendure and B. O'Roak for details regarding *ADNP* molecular inversion probe design. E.E.E. is an investigator of the Howard Hughes Medical Institute.

AUTHOR CONTRIBUTIONS

The study was designed and the results were interpreted by A.T.V.-v.S., B.B.A.d.V., T.K., B.P.C., E.E.E., C.H., G.V., N.V.d.A. and R.F.K. Subject ascertainment and recruitment were carried out by A.T.V.-v.S., J.H.M.S.-H., C.L.M., M.H.W., B.B.A.d.V., T.K., C.R., J.v.d.E., N.V.d.A., A.N., G.A., M.B. and M.W. Sequencing, validation and genotyping were carried out and interpreted by C.H., L.R., G.V., H.M., K.T.W., P.B., B.P.C., L.E.L.M.V., M.F., K.T.W. and H.G.Y. The manuscript was drafted by C.H., G.V., N.V.d.A. and R.F.K. All authors contributed to the final version of the paper.

COMPETING FINANCIAL INTERESTS

The authors declare competing financial interests: details are available in the [online version of the paper](#).

Reprints and permissions information is available online at <http://www.nature.com/reprints/index.html>.

- Autism and Developmental Disabilities Monitoring Network. Prevalence of autism spectrum disorders—Autism and Developmental Disabilities Monitoring Network, 14 sites, United States, 2008. *MMWR Surveill. Summ.* **61**, 1–19 (2012).
- O'Roak, B.J. *et al.* Sporadic autism exomes reveal a highly interconnected protein network of *de novo* mutations. *Nature* **485**, 246–250 (2012).
- Neale, B.M. *et al.* Patterns and rates of exonic *de novo* mutations in autism spectrum disorders. *Nature* **485**, 242–245 (2012).
- Yu, T.W. *et al.* Using whole-exome sequencing to identify inherited causes of autism. *Neuron* **77**, 259–273 (2013).
- Sanders, S.J. *et al.* *De novo* mutations revealed by whole-exome sequencing are strongly associated with autism. *Nature* **485**, 237–241 (2012).
- O'Roak, B.J. *et al.* Exome sequencing in sporadic autism spectrum disorders identifies severe *de novo* mutations. *Nat. Genet.* **43**, 585–589 (2011).
- Devlin, B. & Scherer, S.W. Genetic architecture in autism spectrum disorder. *Curr. Opin. Genet. Dev.* **22**, 229–237 (2012).
- de Light, J. *et al.* Diagnostic exome sequencing in persons with severe intellectual disability. *N. Engl. J. Med.* **367**, 1921–1929 (2012).
- Rauch, A. *et al.* Range of genetic mutations associated with severe non-syndromic sporadic intellectual disability: an exome sequencing study. *Lancet* **380**, 1674–1682 (2012).
- Yang, Y. *et al.* Clinical whole-exome sequencing for the diagnosis of mendelian disorders. *N. Engl. J. Med.* **369**, 1502–1511 (2013).
- Vissers, L.E.L.M. *et al.* A *de novo* paradigm for mental retardation. *Nat. Genet.* **42**, 1109–1112 (2010).
- Gillberg, C. & Billstedt, E. Autism and Asperger syndrome: coexistence with other clinical disorders. *Acta Psychiatr. Scand.* **102**, 321–330 (2000).
- Pinto, D. *et al.* Functional impact of global rare copy number variation in autism spectrum disorders. *Nature* **466**, 368–372 (2010).
- Talkowski, M.E. *et al.* Sequencing chromosomal abnormalities reveals neurodevelopmental loci that confer risk across diagnostic boundaries. *Cell* **149**, 525–537 (2012).
- Iossifov, I. *et al.* *De novo* gene disruptions in children on the autistic spectrum. *Neuron* **74**, 285–299 (2012).
- O'Roak, B.J. *et al.* Multiplex targeted sequencing identifies recurrently mutated genes in autism spectrum disorders. *Science* **338**, 1619–1622 (2012).
- Mandel, S., Spivak-Pohis, I. & Gozes, I. *ADNP* differential nucleus/cytoplasm localization in neurons suggests multiple roles in neuronal differentiation and maintenance. *J. Mol. Neurosci.* **35**, 127–141 (2008).
- Vulih-Shultzman, I. *et al.* Activity-dependent neuroprotective protein snippet NAP reduces tau hyperphosphorylation and enhances learning in a novel transgenic mouse model. *J. Pharmacol. Exp. Ther.* **323**, 438–449 (2007).
- Abecasis, G.R. *et al.* An integrated map of genetic variation from 1,092 human genomes. *Nature* **491**, 56–65 (2012).
- Gozes, I. *et al.* NAP: research and development of a peptide derived from activity-dependent neuroprotective protein (*ADNP*). *CNS Drug Rev.* **11**, 353–368 (2005).
- Bassan, M. *et al.* Complete sequence of a novel protein containing a femtomolar-activity-dependent neuroprotective peptide. *J. Neurochem.* **72**, 1283–1293 (1999).
- Gozes, I. *et al.* Protection against developmental retardation in apolipoprotein E-deficient mice by a fatty neuropeptide: implications for early treatment of Alzheimer's disease. *J. Neurobiol.* **33**, 329–342 (1997).
- Mandel, S., Rechavi, G. & Gozes, I. Activity-dependent neuroprotective protein (*ADNP*) differentially interacts with chromatin to regulate genes essential for embryogenesis. *Dev. Biol.* **303**, 814–824 (2007).
- Mosch, K., Franz, H., Soeroes, S., Singh, P.B. & Fischle, W. HP1 recruits activity-dependent neuroprotective protein to H3K9me3 marked pericentromeric heterochromatin for silencing of major satellite repeats. *PLoS ONE* **6**, e15894 (2011).
- Smothers, J.F. & Henikoff, S. The HP1 chromo shadow domain binds a consensus peptide pentamer. *Curr. Biol.* **10**, 27–30 (2000).
- Pollard, K.S., Hubisz, M.J., Rosenbloom, K.R. & Siepel, A. Detection of nonneutral substitution rates on mammalian phylogenies. *Genome Res.* **20**, 110–121 (2010).
- Zuker, M. Mfold web server for nucleic acid folding and hybridization prediction. *Nucleic Acids Res.* **31**, 3406–3415 (2003).
- Nagy, E. & Maquat, L.E. A rule for termination-codon position within intron-containing genes: when nonsense affects RNA abundance. *Trends Biochem. Sci.* **23**, 198–199 (1998).
- Schoenberg, D.R. & Maquat, L.E. Regulation of cytoplasmic mRNA decay. *Nat. Rev. Genet.* **13**, 246–259 (2012).
- Kervestin, S. & Jacobson, A. NMD: a multifaceted response to premature translational termination. *Nat. Rev. Mol. Cell Biol.* **13**, 700–712 (2012).
- Dresner, E., Agam, G. & Gozes, I. Activity-dependent neuroprotective protein (*ADNP*) expression level is correlated with the expression of the sister protein *ADNP2*: deregulation in schizophrenia. *Eur. Neuropsychopharmacol.* **21**, 355–361 (2011).
- Zamostiano, R. *et al.* Cloning and characterization of the human activity-dependent neuroprotective protein. *J. Biol. Chem.* **276**, 708–714 (2001).
- Aboonq, M.S., Vasiliou, S.A., Haddley, K., Quinn, J.P. & Bubbs, V.J. Activity-dependent neuroprotective protein modulates its own gene expression. *J. Mol. Neurosci.* **46**, 33–39 (2012).
- Pinhasov, A. *et al.* Activity-dependent neuroprotective protein: a novel gene essential for brain formation. *Brain Res. Dev. Brain Res.* **144**, 83–90 (2003).
- Firth, H.V. *et al.* DECIPHER: database of chromosomal imbalance and phenotype in humans using ensembl resources. *Am. J. Hum. Genet.* **84**, 524–533 (2009).
- Mandel, S. & Gozes, I. Activity-dependent neuroprotective protein constitutes a novel element in the SWI/SNF chromatin remodeling complex. *J. Biol. Chem.* **282**, 34448–34456 (2007).
- Ronan, J.L., Wu, W. & Crabtree, G.R. From neural development to cognition: unexpected roles for chromatin. *Nat. Rev. Genet.* **14**, 347–359 (2013).
- Lessard, J. *et al.* An essential switch in subunit composition of a chromatin remodeling complex during neural development. *Neuron* **55**, 201–215 (2007).
- Kosho, T. *et al.* Clinical correlations of mutations affecting six components of the SWI/SNF complex: detailed description of 21 patients and a review of the literature. *Am. J. Med. Genet.* **161A**, 1221–1237 (2013).
- Santen, G.W. *et al.* Coffin-Siris syndrome and the BAF complex: genotype-phenotype study in 63 patients. *Hum. Mutat.* **34**, 1519–1528 (2013).
- Hoyer, J. *et al.* Haploinsufficiency of *ARID1B*, a member of the SWI/SNF-a chromatin-remodeling complex, is a frequent cause of intellectual disability. *Am. J. Hum. Genet.* **90**, 565–572 (2012).
- Ho, L. & Crabtree, G.R. Chromatin remodelling during development. *Nature* **463**, 474–484 (2010).
- de la Serna, I.L., Carlson, K.A. & Imbalzano, A.N. Mammalian SWI/SNF complexes promote MyoD-mediated muscle differentiation. *Nat. Genet.* **27**, 187–190 (2001).
- Kemper, J.K., Kim, H., Miao, J., Bhalla, S. & Bae, Y. Role of an mSin3A-Swi/Snf chromatin remodeling complex in the feedback repression of bile acid biosynthesis by SHP. *Mol. Cell. Biol.* **24**, 7707–7719 (2004).
- Choi, E.Y., Park, J.A., Sung, Y.H. & Kwon, H. Generation of the dominant-negative mutant of hArpNbeta: a component of human SWI/SNF chromatin remodeling complex. *Exp. Cell Res.* **271**, 180–188 (2001).
- Tsurusaki, Y. *et al.* Mutations affecting components of the SWI/SNF complex cause Coffin-Siris syndrome. *Nat. Genet.* **44**, 376–378 (2012).

ONLINE METHODS

Patients. Patients were selected for inclusion in this study from different cohorts tested on either family-based WES, targeted resequencing or high-resolution melting analysis (Table 1). Clinical evaluation was performed by at least one expert clinical geneticist. Written informed consent for inclusion in the study was obtained for all patients and consent for the publication of photographs was obtained for patients 1, 2, 4, 5, 6 and 8.

Sanger sequencing. Primers were designed using Primer3 (refs. 47,48). PCR was performed using GoTaq polymerase (Promega) on DNA from peripheral blood and on cDNA from lymphoblastoid cells, using standard protocol. Capillary electrophoresis sequencing (ABI 3130 genetic analyzer; Applied Biosystems) was performed using the ABI BigDye terminator V3.1 Cycle Sequencing Kit (Applied Biosystems), following standard protocol. Data was analyzed in CLC DNA Workbench (CLC Bio).

Whole-exome sequencing (WES). Patient 1 was detected in a family-based WES study (C.H., G.V., F.V.N., N.V.d.A. and R.F.K., unpublished data). Patient DNA was fragmented using Covaris M220 Focused-ultrasonicator, followed by TruSeq DNA Sample Preparation (Illumina), enrichment using the SeqCap EZ Human Exome Library v3.0 kit (NimbleGen, Roche), and sequencing on HiSeq 2000 (Illumina), all following standard protocols. Data analysis was performed using Galaxy (see URLs)^{49–51}. Variants were filtered by VariantDB (see URLs) to exclude variants with (i) low quality, using thresholds based on correlation between NGS data and SNP-chip genotyping, (ii) intronic or intergenic location, except splice sites and (iii) inheritance from the parents. WES sequencing of patients 2, 3 and 4 was performed as described^{2,8}. The mutation in patient 5 was identified in a family trio based study. WES was performed using Illumina technology, and sequence data was returned and analyzed using software supplied from Oxford Gene Technology. Presence of reported (*de novo*) mutations were confirmed by an independent technique such as Sanger sequencing. Raw sequence data will be uploaded in The European Genome-phenome Archive (EMBL-EBI) database.

Molecular inversion probes (MIPs). Patients 7, 8 and 9 were discovered from a MIP-based screen of 2,743 probands with intellectual disability and/or ASD. Patient 10 was included from a MIP-based screen of 2,446 patients with autism from the Simon Simplex Collection (SSC)¹⁶. The MIP screening and analysis was performed as previously described, and MIP probe sequences for *ADNP* are available¹⁶. Inheritance determination and validation were performed by Sanger sequencing.

High-resolution melting (HRM). We screened 192 control chromosomes for the presence of the mutations identified in the ten patients using HRM. Primers were designed using the HRMA Assay Design module of Beacon Designer 8.10 (Premier Biosoft). HRM was performed on a LightCycler 480 (Roche) with the LCGreen⁺ incorporating dye (Idaho Technology). Meltcurve analysis was performed by the Gene Scanning module of the LightCycler software.

Samples with deviating curves were analyzed by Sanger sequencing. The mutation in patient 6 was identified using the same protocol, as part of the cohort of 148 probands with idiopathic ASD, for which microarray analysis did not reveal any abnormalities.

Real-time quantitative PCR. RNA isolation, cDNA synthesis and quality control were performed as described earlier⁵². mRNA expression was examined by an optimized three-step real-time quantitative PCR assay following the protocol described before⁵³. Besides *ADNP* itself, *ADNP2* was included based on the reported correlation of expression in human brain tissue³¹. *TMPO*, *CCNC* and *PLAGL2* were reported to be significantly downregulated in homozygous *Adnp* knockout mice embryos, whereas *ABCF3* was reported to be upregulated in heterozygous *Adnp* knockout mice embryos^{18,23}. Finally, *TP53* is upregulated in HT29 cells incubated with *ADNP* antiligodeoxynucleotide³². *YWHAZ* and *HPRT* were selected as reference genes, according to geNorm calculations⁵⁴. qPCR primers were selected from literature^{31,55}, the RTPrimerDB⁵⁶ or designed using an in-house automated pipeline (see URLs), conforming to requirements of intron-spanning location, no SNP content, no dimer formation at the 3' end of the primers, and low amplicon folding, with no folding in primer binding sites. The amplification efficiency of the different primers was assessed and confirmed to be above 1.85. Primer sequences are available on request. Expression values of two cDNA syntheses originating from two different RNA isolations per patient were compared to the values obtained from eight control individuals. Statistical testing was performed using linear mixed models in order to investigate significant differences in expression between the patients compared to controls.

47. Untergasser, A. *et al.* Primer3—new capabilities and interfaces. *Nucleic Acids Res.* **40**, e115 (2012).
48. Koressaar, T. & Remm, M. Enhancements and modifications of primer design program Primer3. *Bioinformatics* **23**, 1289–1291 (2007).
49. Giardine, B. *et al.* Galaxy: a platform for interactive large-scale genome analysis. *Genome Res.* **15**, 1451–1455 (2005).
50. Blankenberg, D. *et al.* Galaxy: a web-based genome analysis tool for experimentalists. *Curr. Protoc. Mol Biol* **89**, 19.10.1–19.10.21 (2010).
51. Goecks, J., Nekrutenko, A., Taylor, J. & Galaxy, T. Galaxy: a comprehensive approach for supporting accessible, reproducible, and transparent computational research in the life sciences. *Genome Biol.* **11**, R86 (2010).
52. Van der Aa, N. *et al.* Fourteen new cases contribute to the characterization of the 7q11.23 microduplication syndrome. *Eur. J. Med. Genet.* **52**, 94–100 (2009).
53. Vandeweyer, G., Van der Aa, N., Reyniers, E. & Kooy, R.F. The contribution of CLIP2 haploinsufficiency to the clinical manifestations of the Williams-Beuren syndrome. *Am. J. Hum. Genet.* **90**, 1071–1078 (2012).
54. Vandesompele, J. *et al.* Accurate normalization of real-time quantitative RT-PCR data by geometric averaging of multiple internal control genes. *Genome Biol* **3**, 34.1–34.11 (2002).
55. Yang, M.C., Weissler, J.C., Terada, L.S., Deng, F. & Yang, Y.S. Pleiomorphic adenoma gene-like-2, a zinc finger protein, transactivates the surfactant protein-C promoter. *Am. J. Respir. Cell Mol. Biol.* **32**, 35–43 (2005).
56. Lefever, S., Vandesompele, J., Speleman, F. & Pattyn, F. RTPrimerDB: the portal for real-time PCR primers and probes. *Nucleic Acids Res.* **37**, D942–D945 (2009).